Photosensitization of coronene–purine hybrids for photodynamic therapy

Amir Hossein Rasouli Amirabadi[a], Mahmoud Mirzaei[a,*]

[a]Department of Medicinal Chemistry, School of Pharmacy and Pharmaceutical Sciences, Isfahan University of Medical Sciences, Isfahan, Iran

Abstract

Photosensitization properties of coronene-purine (Cor-P) hybrids for photodynamic therapy (PDT) have been investigated in this work. Eight hybrid Cor-P models have been designed by the addition of adenine (A) and guanine (G) nucleobase to Cor species. The evaluated absorption and emission energies indicated that the singular models are not good at all for PDT process whereas their hybrid models are very much useful for the purpose. Although the Cor-A models are very much better for visible region, the Cor-G models could also be used in the near-infrared region. The main point of these materials is to generate singlet molecular oxygen, in which all the investigated Cor-P hybrids could supply the required energy for triplet to singlet conversion of molecular oxygen. This work has been done based on the advantage of quantum computation for solving the problems in the living systems.

Keywords: Photodynamic therapy; photosensitizer; coronene; adenine; guanine.

Introduction

Cancer therapy has become the main problem of life scientists for recent years [1]. Although many procedures have been developed for this purpose, cancer is still an uncontrolled process [2]. Photodynamic therapy (PDT) is a therapeutical process based on employing photosensitizers (PS) and extra light source to generate reactive singlet molecular oxygen ($^1O_2$) to kill tumor cells [3]. The PS chemical structures could be excited by radiated light source from ground state (S_0) to the excited state (S_1) during (PS→PS*) transition [4]. Stopping the radiation, the PS* could be relaxed again to PS (PS*→PS) and the absorbed energy could be released again to supply energy resource for $^3O_2 \rightarrow {}^1O_2$ conversion which is used in PDT type–II [5]. It is worthy to note that the S_1 could be relaxed to reach the first triplet state (T_1) and then it could be relaxed again to S_0 state (Scheme 1). Examining the values of absorption energies of $S_0 \rightarrow S_1$ and measuring the nonradiative intersystem relaxation of $S_1 \rightarrow T_1$ and emission energies of $T_1 \rightarrow S_0$ are important for evaluating the efficiency of PS species [6]. To this aim, time–dependent density functional theory (TD–DFT) could prepare a high precise environment to investigate the potency of PS species for PDT applications [7].

*Corresponding author: Mahmoud Mirzaei

Tel: +98 (31) 37927101, Fax: +98 (31) 36680011
E-mail: mdmirzaei@pharm.mui.ac.ir
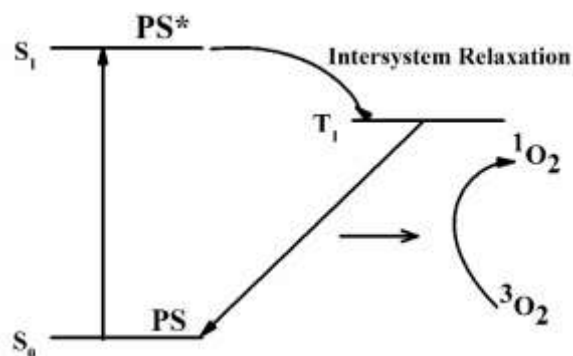
Scheme 1. The PDT type–II process

Biological based chemical structures are always good choices for applications in living systems [8]. Derivatives of nucleobases, including purines and pyrimidines, have shown several advantages for medical applications in human bodies [9–11]. Therefore, specific modifications of nucleobase structures by hybridization with other chemical structures could yield newer applications [12–15]. Coronene (Cor) is a molecular single standing carbon layer, smaller than wide graphene sheets [16]. Since the nanostructures are believed to have novel functions for living systems [17–20], exploring the advantage of coronene–purine (Cor–P) hybrids for PDT could be an interesting task. It is important to note that the major limitation of chemical structures for PDT applications is their absorption (PS*→PS) wavelength range to be in the therapeutic window of 400–850 nm [21]. Afterwards, the emitted wavelength of PS*→PS relaxation which could be considered in the PDT type–II applications for $^3O_2→^1O_2$ conversion requires 0.98 eV [22].

Within this work, we have investigated photosensitization of coronene–purine hybrids for PDT applications based on the advantage of quantum TD–DFT approach for solving problems in living systems. The properties for PS→PS* absorption and

PS*→PS emission have been recognized to show the capability of investigated hybrids for PDT type–II applications.
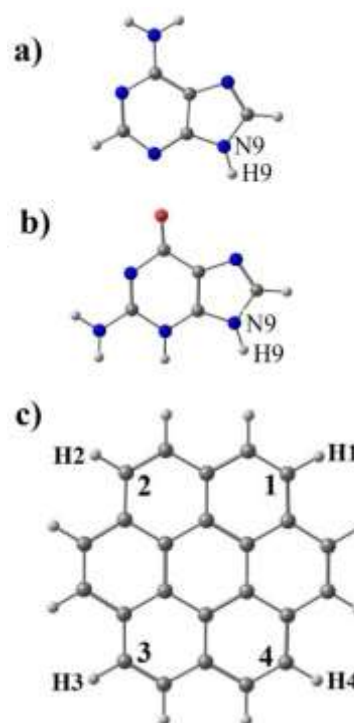
Figure 1. The singular models; a) Adenine, b) Guanine, c) Coronene

Computational details

First, singular structures of Cor (coronene), and P (purine); A (adenine) and G (guanine), have been downloaded from the ChemSpider [23] data bank as they have been separately optimized to obtain minimum energy geometries. Second, Cor–P hybrid models have been designed by

removing one hydrogen atom from N9 atomic site of P and one, two, and four hydrogen atoms from corners of Cor sheet, respectively (Figure 1). The hybrid models including Cor–P1 (Cor and one P), Cor–P2 (Cor and two Ps), Cor–P3 (Cor and two Ps) and Cor–P4 (Cor and four Ps) have been optimized again to obtain minimum structures. Subsequently, TD calculations have been performed to evaluate photosensitization of the investigated models in singular and hybrid forms.

The energies and wavelengths of vertical $S_0 \rightarrow S_1$ absorption, intersystem $S_1 \rightarrow T_1$ relaxation and $T_1 \rightarrow S_0$ emission have been evaluated for the models (Table 1). Moreover, the highest occupied and the lowest unoccupied molecular orbital (HOMO and LUMO) distribution patterns have been demonstrated for the models (Figure 2). Quantum DFT calculations of this work have been done by the standard B3LYP/3–21G* method of the Gaussian program [24].

**Table 1.** Transition information of the singular and hybrid models[*]

Compounds	$S_0 \rightarrow S_1$		$S_1 \rightarrow T_1$	$T_1 \rightarrow S_0$	
	ΔE (eV)	λ (nm)	ΔE (eV)	ΔE (eV)	λ (nm)
A	3.98	312	–0.32	–3.66	368
G	3.82	325	–0.40	–3.42	362
Cor	2.94	421	–0.48	–2.46	503
Cor–A1	2.78	445	–0.37	–2.41	515
Cor–A2	2.66	466	–0.30	–2.36	525
Cor–A3	2.68	463	–0.34	–2.34	529
Cor–A4	2.49	498	–0.24	–2.25	550
Cor–G1	1.71	726	–0.02	–1.69	734
Cor–G2	1.48	836	–0.01	–1.47	840
Cor–G3	1.44	862	–0.02	–1.42	872
Cor–G4	1.08	1143	–0.01	–1.07	1150

[*]Positive energies of $S_0 \rightarrow S_1$ are for absorption, negative energies of $S_1 \rightarrow T_1$ are for intersystem relaxation, negative energies of $T_1 \rightarrow S_0$ are for emission.

Results and discussion

Photosensitization of Cor–P hybrids have been investigated in this work. To this aim, energies of absorption, intersystem relaxation and emission have been evaluated for three singular and eight hybrid models. To prepare hybrids, one, two, and four P counterparts have been respectively added to Cor species to make Cor–P models (Figure 1). The structures have been first optimized and their energies transitions have been subsequently evaluated (Table 1). Moreover, HOMO and LUMO distribution patterns (Figure 2) have been demonstrated to see the orbital situations for electron transitions during absorption and emission process.
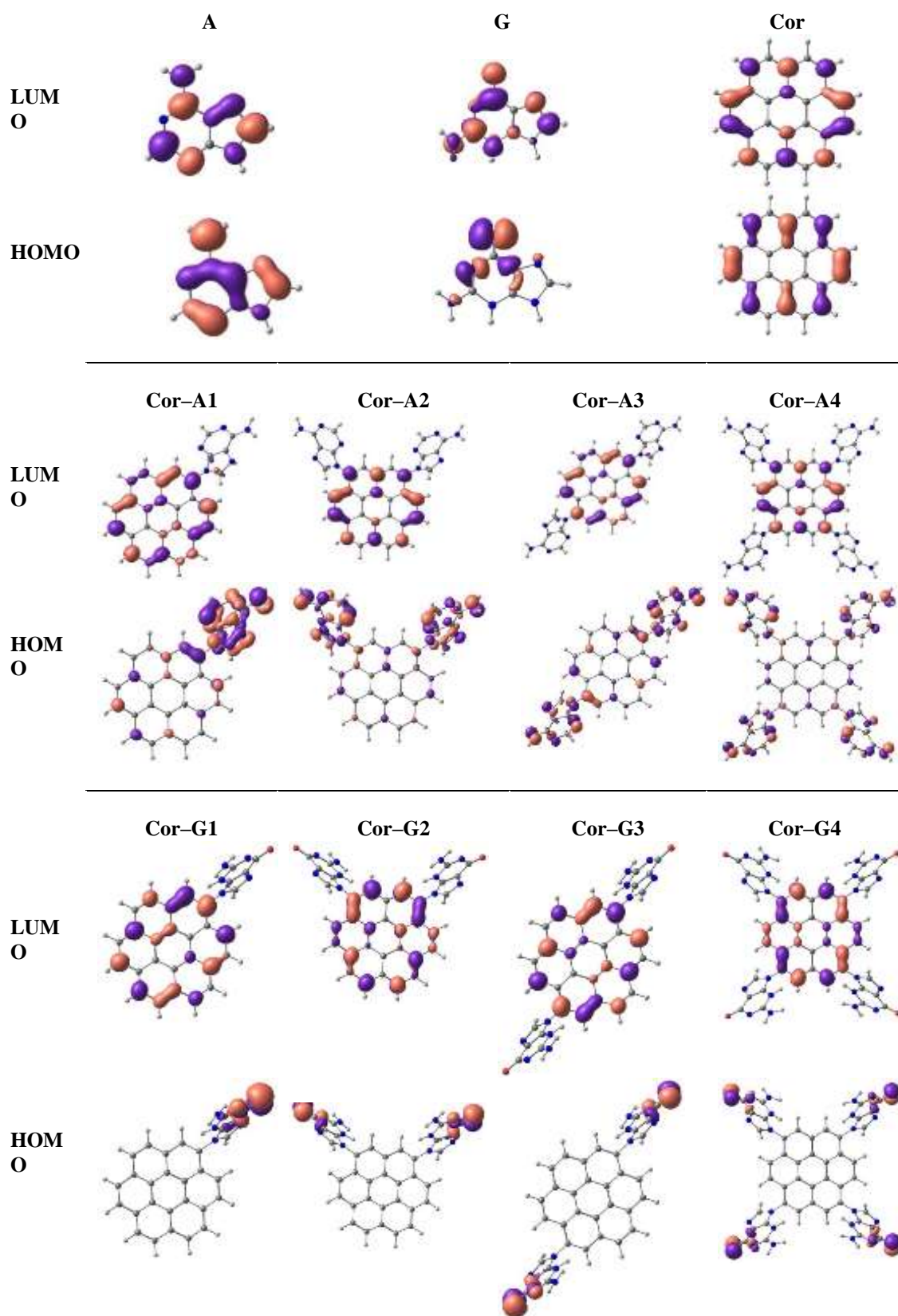
Figure 2. HOMO and LUMO distribution patterns for Cor, A and G singular models and Cor–P hybrid models

Photosensitizers have important roles in PDT process and their characteristic properties could be very well recognized by the evaluated transition energies of quantum TD–DFT calculations [25]. A quick look at the results of Table 1 could reveal the importance of Cor and P hybridization to achieve better $S_0{\rightarrow}S_1$ absorption wavelength properties of photosensitization. While both A and G have absorption wavelengths lower than 400 nm and Cor has 421 nm, the wavelength of hybrids goes to higher fields. The absorption wavelengths are between 445–498 nm for Cor–A hybrids as they are between 726–1143 nm for Cor–G hybrids. Two important notes could be mentioned here; first, number of P groups could increase the absorption wavelength; second, type of P could significantly increase the absorption wavelength. The singular Cor is originally an inorganic material with 420 nm absorption wavelength, in which it could not be easily used in living systems. Both of A and G are very popular for living systems [26,27], but their absorption wavelengths are not good at all for PDT process. Within these results, the importance of chemical functionalization to yield novel applications could be very well recognized as the wavelengths of hybrid structures are significantly different from each of singular Cor, A and G model systems. Moreover, the number of functional group and its type are also important for the modified structure with the specific purpose.

Examining the values of intersystem relaxation energies of $S_1{\rightarrow}T_1$ could indicate that the singular Cor, A and G models and the Cor–A hybrids are preferred for phosphorescence but the Cor–G models are better for fluorescence as indicated by very small magnitudes of intersystem relaxation energies. Interestingly, the Cor–G4 hybrid could be candidate for application in near–infrared region, which is not seen for any of Cor–A hybrids. There are still so many mysteries inside the nucleobases, in which it could be seen here that the A and G species have different effects on the coronene counterpart. Then based on the required energy for penetration into tumor tissue during PDT process, each of hybrid models could be candidate for the purpose. Another important note is that the emission energies of $T_1{\rightarrow}S_0$ for all hybrid models are larger than 0.98 eV of $^3O_2{\rightarrow}^1O_2$ conversion, which enables the investigated hybrids for photosensitizing applications in PDT type–II. The advantages of molecular–scale studies are seen here to make judgments about chemicals.

Careful examining the HOMO–LUMO distribution patterns (Figure 2) could somehow clarify the mystery of A and G nucleobases insides for their different effects on Cor species. The HOMO–LUMO patterns of A are almost located at the similar molecular positions whereas those of G are in different positions. The patterns for Cor are almost similar to those of A, in which the HOMO and LUMO are distributed into similar molecular positions. After hybridization, the HOMO–LUMO are distributed in both Cor and A parts of COR–A hybrids whereas the HOMO is only distributed in the G part and the LUMO is only distributed in the Cor part of Cor–G hybrids. This is maybe the reason of too much significant change of absorption wavelengths for Cor–A and Cor–G hybrids. It could be mentioned here again that the A and G groups could provide better Cor–based hybrid materials for PDT applications in living systems.

Conclusion

Based on the evaluated absorption and emission energies for the Cor, A and G singular models and the Cor-A and Cor-G hybrid models, some trends could be concluded. First, the singular A, G and Cor models are not favorable for PDT processes because of their absorption wavelength ranges. Second, both Cor-A and Cor-G hybrid models could be employed in the PDT processes because of their safe absorption energy wavelengths of therapeutic window. Third, number and type of additional nucleobase could yield different properties for the constructed hybrids. Fourth, the Cor-A hybrids are in the visible region whereas the Cor-G hybrids could also be employed in the near-infrared region. Finally, the emission energies of Cor-A and Cor-G hybrids are larger than 0.98 eV, both of them could be employed for the $^3O_2 \rightarrow {}^1O_2$ conversion of PDT type-II.

Acknowledgments

Author contributions

Both authors have equivalent contribution for this manuscript evaluation.

References

[1] H. Louis, G.K. Fidelis, T.T. Fidelis, S. Onoshe, *J. Med. Chem. Sci.,* **2019**, *2,* 59-63.

[2] L.F. Valverde, D.C. Francisco, R.N. Marcela, M.A. Virginia, M.T. Elizabeth, L.R. Maria, G.C. Elodia, P.G. Eduardo, H.H. Lenin, A.J. Alondra, C.T. Jhair, *Chem. Method.,* **2019**, *3,* 194-210.

[3] H. Abrahamse, M.R. Hamblin, *Biochem. J.,* **2016**, *473,* 347-364.

[4] F. Ponte, G. Mazzone, N. Russo, E. Sicilia, *J. Mol. Model.,* **2018**, *24,* 183-189.

[5] J. Pirillo, G. Mazzone, N. Russo, *Chem.–A Eur. J.,* **2018**, *24,* 3512-3519.

[6] G. Mazzone, A.D. Quartarolo, N. Russo, *Dyes Pig.,* **2016**, *130,* 9-15.

[7] G. Mazzone, M.E. Alberto, B.C. De Simone, T. Marino, N. Russo, *Molecules,* **2016**, *21,* 288-292.

[8] C. Bock, M. Farlik, N.C. Sheffield, *Trends Biotechnol.,* **2016**, *34,* 605-608.

[9] M. Nabati, M. Kermanian, H. Mohammadnejad-Mehrabani, H.R. Kafshboran, M. Mehmannavaz, S. Sarshar, *Chem. Method.,* **2018**, *2,* 128-140.

[10] R.K. Bommeraa, R. Merugu, L. Eppakayala, *Chem. Method.,* **2019**, *3,* 354-361.

[11] Z.U.H. Khan, A. Khan, P. Wan, A.U. Khan, K. Tahir, N. Muhammad, F.U. Khan, H.U. Shah, Z.U. Khan, *Nat. Prod. Res.,* **2018**, *32,* 1161-1169.

[12] M. Mirzaei, H.R. Kalhor, N.L. Hadipour, *J. Mol. Model.* **2011**, *17,* 695-699.

[13] M. Mirzaei, H.R. Kalhor, N.L. Hadipour, *IET Nanobiotechnol.,* **2011**, *5,* 32-35.

[14] M. Mirzaei, S. Ravi, M. Yousefi, *Superlat. Microstruct.,* **2012**, *52,* 306-311.

[15] M. Mirzaei, *Int. J. Nano Dimen.,* **2013**, *3,* 175-179.

[16] K. Harismah, M. Mirzaei, R. Moradi, *Z. Naturforsch. A,* **2018**, *73,* 685-691.

[17] A. Hameed, G.R. Fatima, K. Malik, A. Muqadas, M. Fazal-ur-Rehman, *J. Med. Chem. Sci.,* **2019**, *2,* 9-16.

[18] E. Naderi, M. Mirzaei, L. Saghaie, G. Khodarahmi, O. Gülseren, *Int. J. Nano Dimen.,* **2017**, *8,* 124-131.

[19] A. Kouchaki, O Gülseren, N Hadipour, M Mirzaei, *Phys. Lett. A,* **2016**, *380,* 2160-2166.

[20] M. Mirzaei, R.S. Ahangari, *Superlat. Microstruct.,* **2014**, *65,* 375-379.

[21] N. Mehraban, H.S. Freeman, *Materials,* **2015**, *8,* 4421-4456.

[22] M.E. Alberto, B.C. De Simone, G. Mazzone, E. Sicilia, N. Russo, *Phys. Chem. Chem. Phys.,* **2015**, *17,* 23595-23601.

[23] H.E. Pence, A. Williams, *Chem. Edu. Today,* **2010**, *87,* 1123-1124.

[24] M.J. Frisch, G.W. Trucks, H.B. Schlegel, G.E. Scuseria, M.A. Robb, J.R. Cheeseman, G. Scalmani, V. Barone, B. Mennucci, G.A. Petersson, H. Nakatsuji, M. Caricato, X. Li, H.P. Hratchian, A.F. Izmaylov, J. Bloino, G. Zheng, J.L. Sonnenberg, M. Hada, M. Ehara, K. Toyota, R. Fukuda, J. Hasegawa, M. Ishida, T. Nakajima, Y. Honda, O. Kitao, H. Nakai, T. Vreven, J.A. Montgomery, J.E. Peralta, F. Ogliaro, M. Bearpark, J.J. Heyd, E. Brothers, K.N. Kudin, V.N. Staroverov, R. Kobayashi, J. Normand, K. Raghavachari, A. Rendell, J.C. Burant, S.S. Iyengar, J. Tomasi, M. Cossi, N. Rega, J.M. Millam, M. Klene, J.E. Knox, J.B. Cross, V. Bakken, C. Adamo, J. Jaramillo, R. Gomperts, R.E. Stratmann, O. Yazyev, A.J. Austin, R. Cammi, C. Pomelli, J.W. Ochterski, R.L. Martin, K. Morokuma, V.G. Zakrzewski, G.A. Voth, P. Salvador, J.J. Dannenberg, S. Dapprich, A.D. Daniels, O. Farkas, J.B. Foresman, J.V. Ortiz, J. Cioslowski, D.J. Fox, Gaussian 09, Revision A.01., Gaussian Inc., Wallingford, CT **2009**.

[25] A.H.R. Amirabadi, M. Mirzaei, *Iran. Chem. Commun.,* **2019**, *7,* 223-227.

[26] M. Mirzaei, M. Yousefi, *Superlat. Microstruct.,* **2012**, *52,* 612-617.

[27] B.V.S.K. Chakravarthi, M.T. Goswami, S.S. Pathi, M. Dodson, D.S. Chandrashekar, S. Agarwal, S. Nepal, S.A.H. Balasubramanya, J. Siddiqui, R.J. Lonigro, A.M. Chinnaiyan, L.P. Kunju, N. Palanisamy, S. Varambally, *Prostate*, **2018**, *78*, 693-694.